

# Propofol Detection with Metal Oxide Semiconductor Gas Sensors

*Christian Bur, Henrik Lensch, and Andreas Schütze*

*Lab for Measurement Technology, Saarland University, Saarbrücken, Germany*

*contact: c.bur@lmt.uni-saarland.de*

## Introduction

Breath analysis as a non-invasive tool has the potential to become a powerful tool for early detection and monitoring of diseases. Of great interest is the detection of cancer, diabetes, pulmonary diseases, renal dysfunction, and COPD (chronic obstructive pulmonary disease) [1] as well as early detection of sepsis and inflammation [2]. There are already some biomarkers identified and linked to certain diseases, like acetone for diabetes, hydrogen for lactose intolerance, or nitrous gases for asthma [3], [4]. However, in many cases there is not a single biomarker but rather changes in the concentration of multiple exhaled volatile organic compounds (VOCs) which need to be detected. For cancer detection, changes in VOC profiles between a test and a reference group have frequently been studied [5]. In the breath of healthy humans more than 800 different VOCs have been found [6] with concentrations ranging from several ppt (parts per trillion) up to a few ppm (parts per million). Table 1 summarized major compounds of human breath. Besides endogenous sources of VOCs the inhaled air also has a significant impact on the composition of the exhaled air [7]–[9]. Besides early detection of diseases, the analysis of exhaled air can be used for drug monitoring with the aim to correlate the breath concentration of the given drug or a metabolite to the plasma concentration [10]. The large number of VOCs together with a wide range of concentrations of different target substances poses a serious challenge for the measurement system.

Several techniques have been studied for breath analysis with analytical methods like gas chromatography coupled with mass spectrometry (GC/MS) being the gold standard due its high sensitivity and selectivity. For real time analysis Selected Ion Flow Tube MS (SIFT-MS) or Proton Transfer Reaction MS (PTR-MS) are used [4]. However, these instruments are complex, high-end priced and require trained personnel so that they are mostly used for research purposes.

In drug monitoring, bedside, non-invasive, and ideally online monitoring of exhaled air could have a high therapeutic relevance calling for more cost-effective technologies.

For the intravenous anesthetic propofol, ion mobility spectrometry (IMS) has been studied intensively [11]–[13]. A correlation of the concentration in exhaled air to the plasma concentration was reported [14] and a pharmacokinetic model was suggested to predict the time-delayed and exhaled concentration of propofol [15].

Another promising technology are semiconductor gas sensors based on metal oxides (MOS). Being low-cost, small sized with low power consumption, and easy to integrate make them highly attractive for portable and simple to use hand-held devices [16]. These could also be used in non-clinical environments, i.e., medical practices or even at home.

Besides being highly sensitive, MOS-sensors are non-selective. By using temperature-cycled operation (TCO) [17] we could show that a single MOS sensor is capable of quantifying single VOCs in the low ppb-range in a complex and varying background of interfering VOCs, hydrogen (H<sub>2</sub>) and carbon monoxide (CO), e.g. for indoor air quality applications [18]–[20]. Dynamic operation together with signal processing based on machine learning and a complex lab calibration with randomized gas mixtures are the basis to achieve a performance of MOS sensors which is comparable to analytics but with the advantage of being low-cost and offering real time and online monitoring.

To demonstrate the potential of MOS sensors for drug monitoring, two commercially available MOS sensors, i.e. ZMOD4410 (indoor air sensor) and ZMOD4510 (outdoor air sensor) from Renesas, Dresden,

**Tab. 1:** Major compounds in exhaled breath. After [25], [26].

compound	Concentration range
Hydrogen, H <sub>2</sub>	~ 5000 ppb
Carbon monoxide, CO	0-6000 ppb
Ammonia, NH <sub>3</sub>	500 – 2000 ppb
Acetone, C <sub>3</sub> H <sub>6</sub> O	240 – 1800 ppb
Isoprene, C <sub>5</sub> H <sub>8</sub>	12 – 500 ppb
Ethanol, C <sub>2</sub> H <sub>5</sub> OH	30 – 1000 ppb
Methanol, CH <sub>3</sub> OH	30 – 2000 ppb
n-Propanol, C <sub>3</sub> H <sub>7</sub> OH	0 – 1200 ppb
Iso-Propanol, C <sub>3</sub> H <sub>8</sub> O	0 – 250 ppb
Hydrogen sulfide, H <sub>2</sub> S	0 – 1300 ppb
Nitric oxide, NO	10 - 50 ppb
Methane, CH <sub>4</sub>	2000 – 10,000 ppb
Rel. humidity, H <sub>2</sub> O	~ 90 % @ 35 °C

Germany, are studied in this work for propofol quantification in a simulated atmosphere under lab conditions.

## Methods and Experimental Setup

The sensors are characterized for propofol detection in two calibration measurements simulating a breath atmosphere. Table 2 shows the concentrations of the involved background substances as well as the concentration range of propofol. In measurement 1 ethanol and the level of relative humidity are varied, whereas the concentrations of carbon monoxide and nitric oxide are altered in measurement 2. A custom-made gas mixing system based on mass flow controllers (MFCs, MF-1 from MKS, Munich, Germany) was used for all measurement as described in [21], [22]. Background gases are supplied by gas cylinders whereas propofol is provided by a permeation oven (Dynacalibrator 150 from VICI International, Schenkon, Switzerland). The oven was heated at 70 °C and flushed with 50 ml/min dry synthetic air. To quickly adjust the concentration, an injection MFC was placed downstream of the oven. The concentration range of propofol was 5 ppb to 30 ppb. Each exposure lasted for 60 min followed by a 120 min pause. Different propofol concentrations are applied in a pseudo-randomized fashion.

Temperature cycled operation (TCO) is used to increase the selectivity of the sensors and boost the sensitivity further [23]. A generic temperature cycle consisting of twelve temperature steps in the range of 100 °C to 375 °C with a duration of 7 s and a 5 s high temperature phase at 400 °C between each step is applied, cf. Fig. 1. This results in a total cycle length of 144 s. For control and read-out of the sensors an inhouse built sensor platform based on a microcontroller board (Teensy 4.0, Pjrc.com LLC, Sherwood, Oregon, USA) and communicating with the sensors via I2C at a sampling rate of 10 Hz is used. A detailed description of the hardware can be found elsewhere [24].

**Tab. 2:** Substances and concentrations used in characterization measurements.

compound	measurement 1	measurement 2
H <sub>2</sub>	---	5000 ppb
CO	---	0, 3000, 5000 ppb
Acetone	1000 ppb	1000 ppb
Isoprene	200 ppb	200 ppb
Ethanol	500 ppb, 1000 ppb	500 ppb
Methanol	500 ppb	500 ppb
n-Propanol	50 ppb	50 ppb
Iso-Propanol	20 ppb	20 ppb
H <sub>2</sub> S	20 ppb	20 ppb
NO	---	0, 10, 25, 40 ppb
r.h. @ 20 °C	60, 70, 80 %	80 %
Propofol	20, 15, 25, 5, 30 ppb	20, 15, 25, 5, 10 ppb

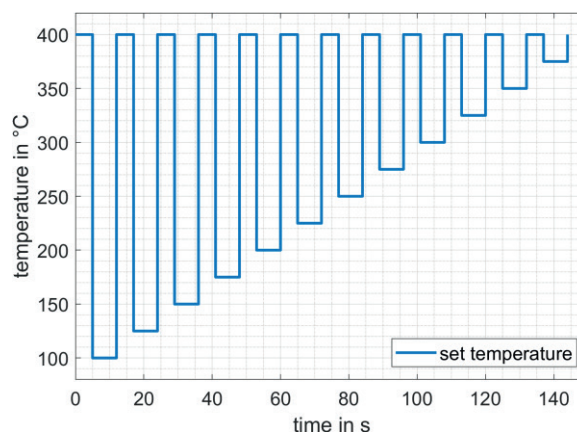


**Fig. 1:** Used temperature cycle. consisting of twelve high and low temperature phases with a total length of 144 s.

The sensor conductance of a temperature cycled gas sensor can be represented as a two-dimensional dataset, where one axis represents a temperature cycle as shown in Fig. 4 and the other dimension represents a so-called quasistatic sensor response shown in Fig. 2 (top). With the temperature cycle as shown in Fig. 1 and the sample rate of 10 Hz the dimension of that two-dimensional matrix is  $N \times 1440$  where  $N$  represents the number of recorded cycles. One way of visualizing the data is plotting the quasi-static sensor response. The quasi-static sensor response takes one data point at the same index of each cycle (i.e. out of 1440) and plots these values over time (i.e. plotting a specific column of the data matrix). This results in a sensor response similar to constantly heated sensors where the various gas exposures can be observed. Since the cycle covers a broad temperature range, there are several quasi-static responses, each corresponding to a specific temperature.

A second way of visualizing TCO data is by selecting a few cycles (i.e. rows of the data matrix) out of the measurement where each cycle is from a different gas mixture. This highlights the transient behavior due to changes in temperature and the corresponding reaction to the gas mixture.

For data evaluation each temperature cycle is divided into 1 s long intervals, in which the mean value and the slope are calculated and extracted as shape describing features, resulting in 288 features per cycle and sensor. In a second step, these features are standardized (z-scored) and used to train a partial least squares regression (PLSR) model. In order to determine the optimal number of PLSR components and to validate the model to prevent overfitting, group-based leave one out cross-validation (LOOCV) is used. Group-based means that an entire exposure (consisting of almost 25 observations, i.e. cycles) is omitted during training and only used for validation.

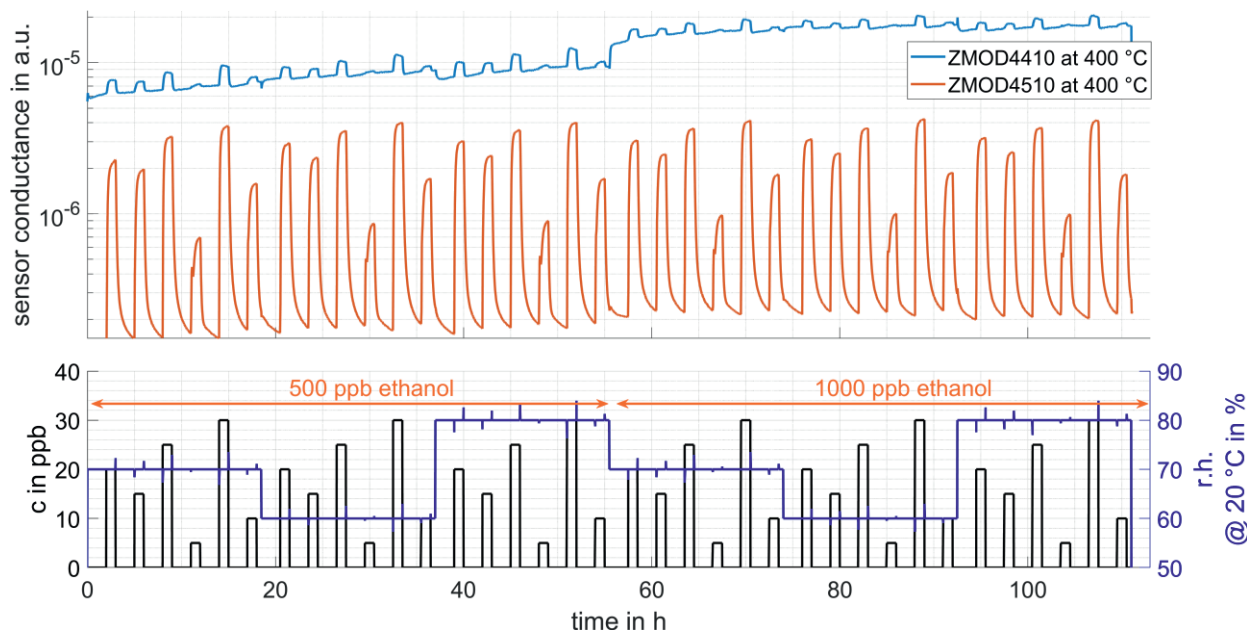


**Fig. 2:** Quasi-static sensor response of the ZMOD4410 and ZMOD4510 at 400 °C for calibration measurement 1 (top) and applied gas profile with varying level of humidity and ethanol (bottom).

## Results

In a first step, the sensor responses of the ZMOD4410 and the ZMOD4510 to the gas profiles in both measurements are studied.

After that, a PLSR model is built to quantify propofol independent of the background mixture.

### Quasi-static sensor response

In a first calibration measurement the concentration of ethanol as one of the main interfering gases as well as the level of relative humidity was varied. The

sensors are exposed to five propofol concentrations in a constant background of acetone, isoprene, methanol, 1- and 2-propanol, and hydrogen sulfide, cf. Tab. 2 second column and Fig. 1 lower part. The quasi-static sensor response at 400 °C of the ZMOD4410 and ZMOD4510 is given in the upper part of Fig. 2. Both sensors show a fast and high response to propofol and are not much affected by the change of humidity. Only the ZMOD4410 reacts to the change in ethanol concentration. The response of the ZMOD4510 seems stronger compared to the ZMOD4410 but the ZMOD4510 never reaches a steady-state condition during 60 min of propofol

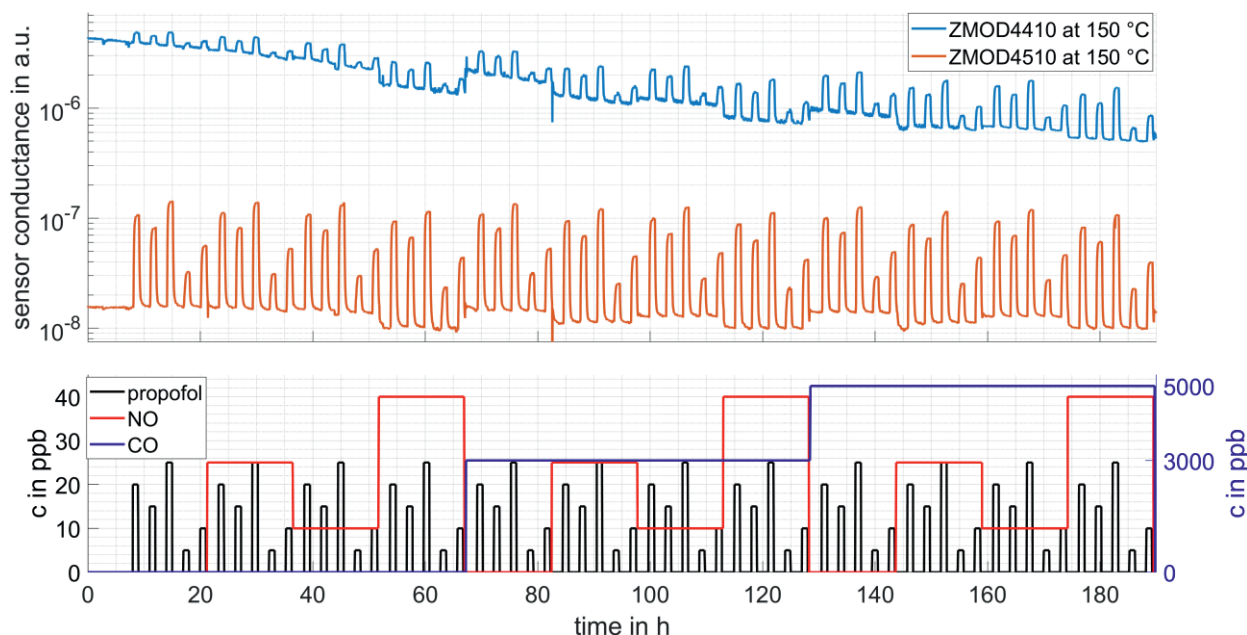


**Fig. 3:** Quasi-static sensor response of the ZMOD4410 and ZMOD4510 at 150 °C for calibration measurement 2 (top) and applied gas profile with varying level of nitric oxide and carbon monoxide (bottom).

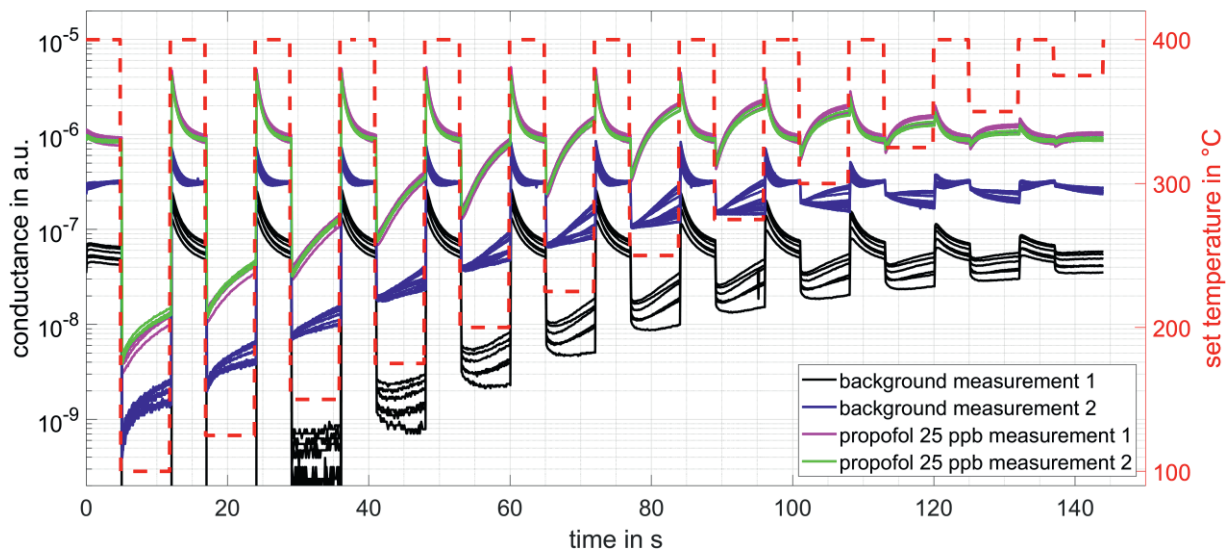


**Fig. 4:** Dynamic sensor response of ZMOD4510 for various background mixtures (i.e. 0 ppb propofol) from measurement 1 and 2 in black and blue, respectively, as well as several cycles in 25 ppb propofol from both measurements in magenta and green. The set temperature is given in red.

exposure. Similarly, when propofol is switched off, the response of the ZMOD4510 drops immediately but never settles on a baseline during 120 min.

The second measurement uses a similar gas profile but instead of ethanol and the level of relative humidity, carbon monoxide and nitric oxide concentrations were changed. Table 2 last column provides the concentrations of each substance. The propofol profile together with the variable interfering gases (CO and NO) is illustrated in the bottom panel of Fig. 3. The purpose of measurement 2 is to study the influence of CO and NO (CO is associated with smokers), on the sensor response of the two air quality sensors. The same sensor samples are used as in measurement 1. Fig. 3 shows the quasi-static sensor response of both sensors at 150 °C. The signal of the ZMOD4510 is more stable compared to the ZMOD4410 with prominent response to the different propofol concentrations. Changes in the NO concentration are clearly visible in both sensor signals.

#### Dynamic sensor response

In addition to the quasi-static sensor response which indicates the sensor response, time constant, baseline stability, and recovery time, the dynamic sensor response reveals the transient behavior when changing the temperature, in particular how the shape of the sensor response is altered by the gas. Thus, the dynamic sensor response provides first insights for the machine learning model since shape-describing feature will be extracted from each temperature cycle which are input to train a regression model. Fig. 4 shows selected cycles in various atmospheres from both measurements. Black and blue cycles represent background only, i.e. 0 ppb propofol, with different levels of humidity, ethanol, nitric oxide, and carbon monoxide. In contrast,

magenta and green cycles correspond to 25 ppb propofol in these different background mixtures. It can clearly be seen that the cycles in propofol are almost perfectly overlapping indicating that the background composition has only a minor influence. Additionally, when comparing the shape of the cycle with and without propofol, a clear difference can be observed, especially for the temperature range 200 °C – 300 °C.

#### Building a Regression Model

In the next step, each cycle is divided into 1 s long intervals, from which the mean and the slope are extracted as shape-describing features. These 576 features (two sensors with two features each and 144 feature segments/intervals) are used as input to train a regression model. For this, the feature data from both measurements are combined and split into a training and test set. The training set consist of all propofol exposures (incl. 0 ppb) from measurement 1

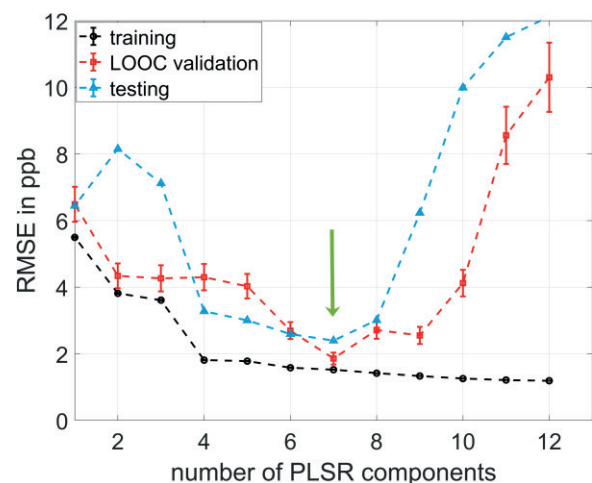


**Fig. 5:** Performance plot of the PLSR model with group based LOOCV for the combined dataset of measurement 1 and 2.

and only background groups, i.e. 0 ppb propofol of measurement 2. The test data holds only the propofol exposures from measurement 2 (5 ppb to 25 ppb). In order to find the optimal number of PLSR components, the performance plot in Fig. 5 is studied. Here, several PLSR models with different number of PLSR components are trained and validated using group-based LOOCV on the training set as well as using (unknown) test data. The optimal number of components is defined just before the validation and testing error increases significantly. Thus, 7 PLSR components are used with RMSE values for training, validation, and testing of 1.5 ppb, 1.9 ppb, and 2.3 ppb respectively (cf. Fig. 5).

#### Prediction of Propofol Concentrations

A PLSR model with 7 components is trained on the training set (measurement 1 and only background groups of measurement 2), cf. Fig. 6. For testing the model, entire measurement 2 is used. Fig. 7 shows the model estimate for measurement 2 (red curve). The true concentration is given in blue. The prediction of the propofol concentration in the range of 0 ppb to 20 ppb is accurate within the range of 2-3 ppb. The lower propofol concentrations (5-15 ppb) are overestimated whereas the highest concentration (25 ppb) is a bit underestimated.

#### Discussion

The results suggest that commercially available MOS sensors, in particular the indoor air sensor ZMOD4410 and the outdoor air sensor ZMOD4510, are suitable candidates for selective quantification of propofol in the relevant concentration range of 0 ppb

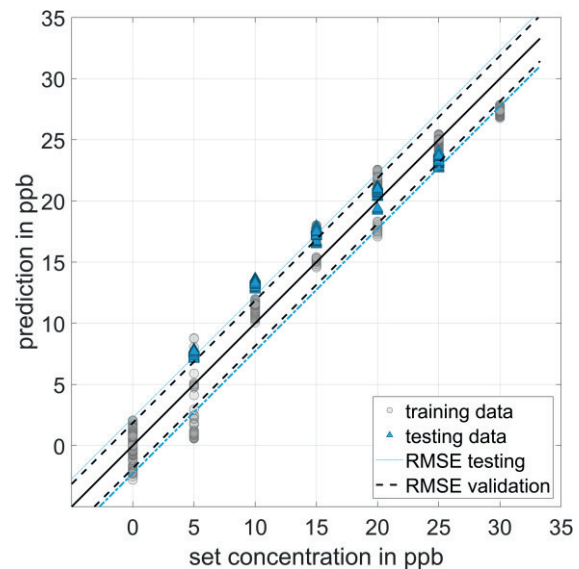


Fig. 6: PLSR plot using 7 components.

to 30 ppb and varying background gases when run in temperature cycled operation and using an advanced machine learning model. Future research will address improvements of the operating mode and data evaluation as well as long-term stability.

#### Acknowledgments

CB gratefully acknowledges the support by the foundation ME-Saar (Anschubfinanzierung MINT) and the support by the Ministry of Finance and Research of the federate state Saarland (Landesforschungsförderung).

Part of this research was funded within project SE-ProEng, financed by the European Regional

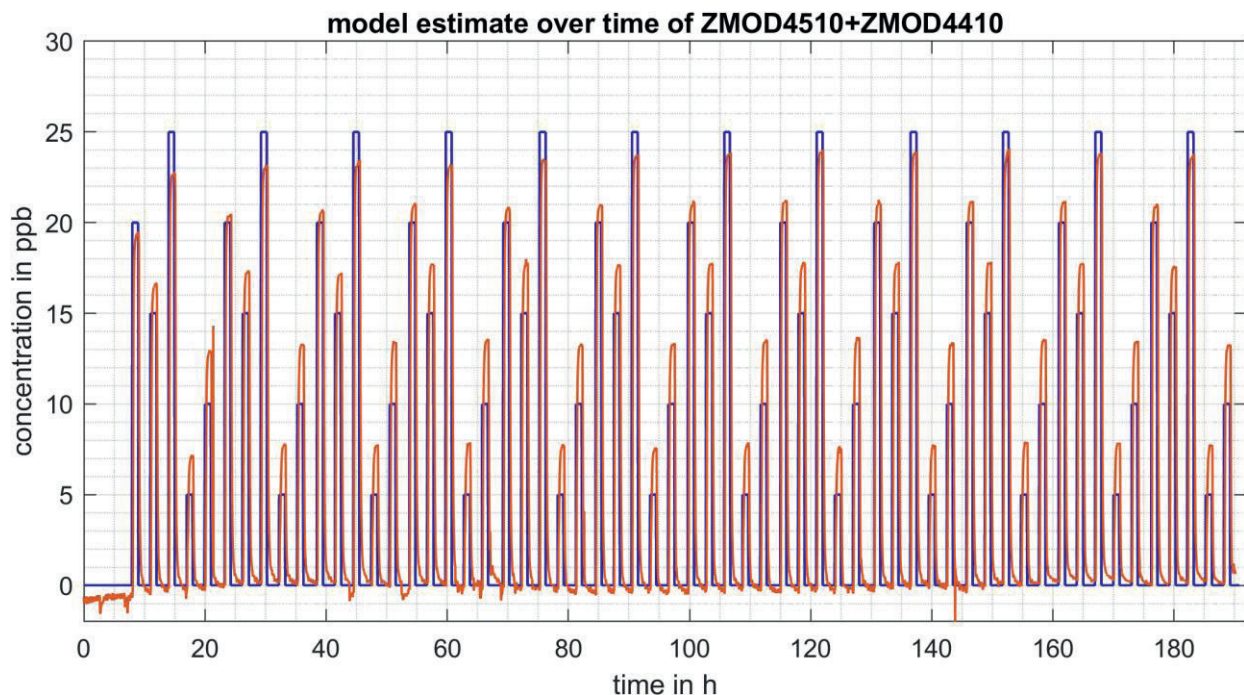


Fig. 7: Model estimate over time of measurement 2 using a PLSR model with 7 components. The model is trained with data from measurement 1 plus background groups, i.e. 0 ppb propofol, from measurement 2.

Development Fund (ERDF), project number 14.2.1.4-2019/1.

## Literature

- [1] J. Pereira *et al.*, “Breath Analysis as a Potential and Non-Invasive Frontier in Disease Diagnosis: An Overview,” *Metabolites* 2015, Vol. 5, Pages 3-55, vol. 5, no. 1, pp. 3–55, Jan. 2015, doi: 10.3390/METABO5010003.
- [2] T. Fink *et al.*, “Volatile organic compounds during inflammation and sepsis in rats: a potential breath test using ion-mobility spectrometry,” *Anesthesiology*, vol. 122, no. 1, pp. 117–126, 2015, doi: 10.1097/ALN.0000000000000420.
- [3] N. Marczin and Magdi. Yacoub, *Disease markers in exhaled breath : basic mechanisms and clinical applications*. IOS Press, NATO Science Series, 2002.
- [4] C. Lourenço and C. Turner, “Breath Analysis in Disease Diagnosis: Methodological Considerations and Applications,” *Metabolites* 2014, Vol. 4, Pages 465-498, vol. 4, no. 2, pp. 465–498, Jun. 2014, doi: 10.3390/METABO4020465.
- [5] A. Krilaviciute, J. A. Heiss, M. Leja, J. Kupcinskas, H. Haick, and H. Brenner, “Detection of cancer through exhaled breath: a systematic review,” *Oncotarget*, vol. 6, no. 36, pp. 38643–38657, 2015, doi: 10.18632/ONCOTARGET.5938.
- [6] B. de Lacy Costello *et al.*, “A review of the volatiles from the healthy human body,” *J Breath Res*, vol. 8, no. 1, p. 014001, Jan. 2014, doi: 10.1088/1752-7155/8/1/014001.
- [7] A. Spatafora-Salazar *et al.*, “Volatile compounds in human breath: critical review and meta-analysis,” *J Breath Res*, vol. 16, no. 2, p. 024001, Feb. 2022, doi: 10.1088/1752-7163/AC5230.
- [8] J. K. Schubert, W. Miekisch, T. Birken, K. Geiger, and G. F. E. Nöldge-Schomburg, “Impact of inspired substance concentrations on the results of breath analysis in mechanically ventilated patients,” <http://dx.doi.org/10.1080/13547500500050259>, vol. 10, no. 2–3, pp. 138–152, Mar. 2008, doi: 10.1080/13547500500050259.
- [9] T. Hüppe *et al.*, “Volatile organic compounds in ventilated critical care patients: A systematic evaluation of cofactors,” *BMC Pulm Med*, vol. 17, no. 1, pp. 1–15, Aug. 2017, doi: 10.1186/S12890-017-0460-0/FIGURES/3.
- [10] L. M. Müller-Wirtz *et al.*, “Exhaled Propofol Concentrations Correlate With Plasma and Brain Tissue Concentrations in Rats,” *Anesth Analg*, vol. 132, no. 1, pp. 110–118, Jan. 2021, doi: 10.1213/ANE.00000000000004701.
- [11] A. Ahrens and S. Zimmermann, “Towards a hand-held, fast, and sensitive gas chromatograph-ion mobility spectrometer for detecting volatile compounds,” *Anal Bioanal Chem*, vol. 413, no. 4, pp. 1009–1016, Feb. 2021, doi: 10.1007/S00216-020-03059-9/TABLES/2.
- [12] T. Fink, J. I. Baumbach, and S. Kreuer, “Ion mobility spectrometry in breath research,” *J Breath Res*, vol. 8, no. 2, p. 027104, Mar. 2014, doi: 10.1088/1752-7155/8/2/027104.
- [13] J. I. Baumbach, “Ion mobility spectrometry coupled with multi-capillary columns for metabolic profiling of human breath,” *J. Breath Res.*, vol. 3, no. 3, pp. 1–16, 2009, doi: 10.1088/1752-7155/3/3/034001.
- [14] F. Maurer *et al.*, “Calibration and validation of a MCC/IMS prototype for exhaled propofol online measurement,” *J Pharm Biomed Anal*, vol. 145, pp. 293–297, Oct. 2017, doi: 10.1016/J.JPBA.2017.06.052.
- [15] S. Kreuer, A. Hauschild, T. Fink, J. I. Baumbach, S. Maddula, and T. Volk, “Two different approaches for pharmacokinetic modeling of exhaled drug concentrations,” *Sci Rep*, vol. 4, Jun. 2014, doi: 10.1038/SREP05423.
- [16] A. T. Güntner, S. Abegg, K. Königstein, P. A. Gerber, A. Schmidt-Trucksäss, and S. E. Pratsinis, “Breath sensors for health monitoring,” *ACS Sens*, vol. 4, no. 2, pp. 268–280, Feb. 2019, doi: 10.1021/acssensors.8b00937.
- [17] A. Schütze and T. Sauerwald, “Dynamic operation of semiconductor sensors,” in *Semiconductor Gas Sensors*, 2nd ed., R. Jaanisio and O. Kiang Tan, Eds. Woodhead Publishing, 2020, pp. 385–412. doi: 10.1016/B978-0-08-102559-8.00012-4.
- [18] T. Baur, J. Amann, C. Schultealbert, and A. Schütze, “Field Study of Metal Oxide Semiconductor Gas Sensors in Temperature Cycled Operation for Selective VOC Monitoring in Indoor Air,” *Atmosphere* 2021, Vol. 12, Page 647, vol. 12, no. 5, p. 647, May 2021, doi: 10.3390/ATMOS12050647.
- [19] Y. Robin, J. Amann, P. Goodarzi, T. Schneider, A. Schütze, and C. Bur, “Deep Learning Based Calibration Time Reduction for MOS Gas Sensors with Transfer Learning,” *Atmosphere* 2022, Vol. 13, Page 1614, vol. 13, no. 10, p. 1614, Oct. 2022, doi: 10.3390/ATMOS13101614.
- [20] Y. Robin *et al.*, “High-Performance VOC Quantification for IAQ Monitoring Using Advanced Sensor Systems and Deep Learning,” *Atmosphere* 2021, Vol. 12, Page 1487, vol. 12, no. 11, p. 1487, Nov. 2021, doi: 10.3390/ATMOS12111487.
- [21] M. Leidinger, C. Schultealbert, J. Neu, A. Schütze, and T. Sauerwald, “Characterization and calibration of gas sensor systems at ppb level—a versatile test gas generation system,” *Meas Sci Technol*, vol. 29, no. 1, p. 015901, Dec. 2017, doi: 10.1088/1361-6501/AA91DA.
- [22] N. Helwig, M. Schüler, C. Bur, A. Schütze, and T. Sauerwald, “Gas mixing apparatus for automated gas sensor characterization,” *Meas Sci Technol*, vol. 25, no. 5, p. 055903, Mar. 2014, doi: 10.1088/0957-0233/25/5/055903.
- [23] T. Baur, A. Schütze, and T. Sauerwald, “Optimierung des temperaturzyklischen Betriebs von Halbleitersensoren,” *tm - Technisches Messen*, vol. 82, no. 4, pp. 187–195, Apr. 2015, doi: 10.1515/TEME-2014-0007.
- [24] C. Fuchs, H. Lensch, O. Brieger, T. Baur, C. Bur, and A. Schütze, “Concept and Realization of a Modular and Versatile Platform for Metal Oxide Semiconductor Gas Sensors,” *tm - Technisches Messen*, vol. in press, 2022.
- [25] J. D. Fenske and S. E. Paulson, “Human breath emissions of VOCs,” *J Air Waste Manag Assoc*, vol. 49, no. 5, pp. 594–598, 1999, doi: 10.1080/10473289.1999.10463831.
- [26] T. L. Mathew, P. Pownraj, S. Abdulla, and B. Pulithadathil, “Technologies for Clinical Diagnosis Using Expired Human Breath Analysis,” *Diagnostics (Basel)*, vol. 5, no. 1, pp. 27–60, 2015, doi: 10.3390/DIAGNOSTICS5010027.